

INFLUENCE OF INPUT MOTION SCALING METHODS ON THE DRIFT RESPONSE OF DECOUPLED SSI DYNAMIC ANALYSIS

Yusuf GÜZEL^{1*}, Fidan GÜZEL²

¹ Faculty of Engineering, Necmettin Erbakan University, No:42/A, KONYA,

ORCID No : <https://orcid.org/0000-0003-2957-8060>

² Faculty of Engineering, Iğdır University, Iğdır,

ORCID No : <https://orcid.org/0000-0002-3204-5305>

Keywords	Abstract
<p>Soil classes Design response spectrum Outcrop/surface motion Nonlinear site response analysis Seismic performance of structures.</p>	<p>Propagation of seismic waves through soil deposits may considerably alter their characteristics at surface. This ultimately influences the seismic performance of structures. The influences of soil deposits are included in seismic codes (e.g. Eurocode 8, EC8) by means of proposed design response spectra for different soil classes used in design or retrofitting of structures. Nevertheless, a smooth design response spectrum cannot always represent spectral response of an actual input motion over an engineering period of interest due to its irregular spectral shape. Subsequently, the seismic performance of a structure may be insufficient when a design response spectrum is used. The interaction between soil and structure may also affect the structural behaviour. This study aims to demonstrate the impact of adoption of input motions and soil deposits with soil classes B, C and D on the seismic behaviour of one-bay, 1-storey structure modelled in OpenSEES For this purpose, two different approaches are chosen; (i) seven input motions recorded on ground surface are modified and applied to the model, (ii) seven outcrop motions are scaled according to EC8 and processed through the ideal soil deposits by conducting nonlinear site response analysis, then applied to the model. The results indicate that the model is exposed to more drift responses when it is on softer soil deposit. In addition, imposing input motions obtained at surface from nonlinear site response analysis cause higher drift responses than directly applying input motions.</p>

DEPREM İVME HAREKETİ ÖLÇEKLENDİRME YÖNTEMLERİNİN SSI DİNAMİK ANALİZİ ÜZERİNDEKİ ETKİSİ

Anahtar Kelimeler	Öz
<p>Zemin sınıfları Tasarım davranış spectrumu Yüzeysel kaya ivme hareketi Doğrusal olmayan zemin analizi Yapıların sismik davranışı</p>	<p>Zemin tabakaları boyunca hareket eden sismik dalgaların özellikleri yüzeye ulaştıklarında önemli ölçüde değişime uğramış olabilir. Bu zemin tabakaları ile sismik dalga arasındaki etkileşim yapıların sismik performansını etkiler. Bu etki, yapıların tasarımında veya güçlendirilmesinde kullanılan farklı zemin sınıfları için önerilen tasarım spektrumları aracılığıyla sismik kodlara (örneğin Eurocode 8, EC8) dahil edilmiştir. Bununla birlikte, standart tasarım davranış spectrumu, gerçek bir deprem ivme hareketinin spektral davranışı düzensiz olduğundan, gerçek bir deprem hareketini tam olarak temsil edemez. Bu nedenle, standart tasarım spectrumu kullanıldığında bir yapının sismik performansı yetersiz olabilir. Ayrıca, zemin-yapı arasındaki etkileşim nedeni ile de yapısal davranış etkilenebilir. Bu çalışma, deprem ivme hareketlerinin, B, C ve D zemin sınıfları dikkate alınarak, OpenSEES'te modellenen tek açıklıklı ve 1 katlı yapının sismik davranışı üzerindeki etkisini göstermeyi amaçlamaktadır. Bu amaçla iki farklı yaklaşım seçilmiştir; (i) zemin yüzeyinde kaydedilen yedi deprem ivme hareketi modifiye edilmesi ve modele uygulanması, (ii) yedi adet yüzeysel kaya deprem ivme hareketinin EC8'e göre</p>

* Sorumlu yazar; e-posta : yusufkurtdereli@hotmail.com



Bu eser, Creative Commons Attribution License (<http://creativecommons.org/licenses/by/4.0/>) hükümlerine göre açık erişimli bir makaledir.

This is an open access article under the terms of the Creative Commons Attribution License (<http://creativecommons.org/licenses/by/4.0/>).

ölçeklendirilmesi ve doğrusal olmayan zemin analizi sayesinde yüzeysel deprem ivme hareketleri elde edilerek modele uygulanmasıdır. Analizlerden elde edilen sonuçlara göre, yapısal modelin daha yumuşak zemin üzerinde olduğunda daha fazla kat ötelenmesine maruz kaldığını göstermektedir. Ek olarak, doğrusal olmayan zemin analizinden yüzeysel elde edilen ivme hareketlerinin uygulanması, doğrudan ivme hareketlerini uygulamaktan daha büyük kat ötelenmelerine neden olmaktadır.

Araştırma Makalesi

Başvuru Tarihi

: 17.10.2021

Kabul Tarihi

: 24.01.2022

Research Article

Submission Date

: 17.10.2021

Accepted Date

: 24.01.2022

1. Introduction

Earthquakes are the inevitable consequence of the tectonic plates movements. These natural events are happening numerous times with different level of magnitudes and, more importantly, they have different impact on the urban environment. In order to minimize the impact of an earthquake on a specific structure, it is necessary to consider various input motions, representing the main characteristics of the seismic event expected at the site, in the design of new buildings or when retrofitting existing ones (CEN, 2005).

The design of a building in seismically active regions clearly requires nonlinear time domain analyses. Most commonly, the building models are modelled as fixed base with single or multi-degree of freedom system and modified input motions are directly applied at the base of the model (direct method). Alternatively, a full numerical model involving the soil deposit, the foundation and the building can be considered in order to take into account the soil-structure interaction (SSI) under dynamic conditions. Instead, in a decoupled approach the bedrock motions are firstly propagated at ground surface in free-field conditions and then used as input motions for a fixed-base structural model. Subsequently, the building model is assessed based on the engineering demand parameters (e.g. inter-storey drift response, roof drift response, etc.) (CEN, 2005; Galasso & Iervolino, 2011). Since, the nonlinear dynamic analysis of buildings are time and cost consuming, the determination of the adequate number of analyses or input motions is vital. The number of input motions to be considered as adequate depends on the efficiency of the scaling method adapted. The number of input motions should be such that the mean response of an EDP does not change significantly with the increase in the input motions and does not reduce the scatter anymore in the response. In this regard, Eurocode 8 (EC8) recommends considering seven input motions in order to account the mean response in the design of buildings.

From this perspective, the selection and modification of input motions are regarded as critical as the modelling of the buildings (Iervolino & Manfredi, 2008). While the selection of the input motions is usually based on the

magnitude and distance hazard distributions of the site under consideration, different scaling methods have been developed to modify them (Shome, Cornell, Bazzurro & Carballo, 1998; Hancock *et al.*, 2006; Ancheta *et al.*, 2013). Particularly, $0.2T_1-2T_1$ scaling, (i.e. EC8), mean squared error (MSE) method, $S_a(T_1)$ scaling and PGA scaling are amongst the most adopted scaling approaches in the engineering practice (CEN, 2005; Kottke and Rathje, 2008; Mazzoni, Hachem & Sinclair, 2012; Tönük, Ansal, Kurtuluş & Çetiner, 2014; Amirzehni, Taiebat, Fin & DeVall, 2015). General practise in the selection of input motions is firstly to determine a target response spectrum representing the seismic intensity level of the site under consideration. Second step is to select and modify suited input motions. The target spectrum will either be constructed in compliance with the seismic design codes (e.g. EC8) or will be obtained from the site response analysis. The later application is suggested when the safety of a structure is crucially important (e.g. nuclear power plant) or when the soil deposits consist of soft soil materials. In EC8, soil classes B and C are regarded as stiff soils and soil class D is regarded as soft soil. However, the suitability of design response spectra for not only soil class D but also for soil classes B and C are in question (Pitilakis, Riga & Anastasiadis, 2012; Pitilakis, Riga & Anastasiadis, 2013). This will favour the site response analysis in the nonlinear dynamic analysis of buildings.

The site response analyses can be performed through frequency-domain equivalent linear (EQL) or time-domain nonlinear (NL) methods considering total or effective stress approaches (Guzel, 2019). The EQL method is based on the exact continuum solution of wave propagation in horizontally layered visco-elastic materials subjected to vertically propagating transient motions (Roesset, 1977). It models the nonlinear variation of soil shear modulus (G) and damping (D) with shear strain through a sequence of linear analyses with iterative update of stiffness and damping parameters. For a given soil layer, G and D are assumed to be constant with time during the shaking. Therefore, an iterative procedure is needed to ensure that the properties used in the linear dynamic analyses are consistent with the level of strain induced in each layer by the input motion (Kramer, 1996). The analysis is

performed adopting a total stress approach. On the contrary, NL approach adopting a numerical time integration scheme and an effective stress approach are capable of fully capturing soil nonlinearity, pore water pressure build-up and consolidation settlements induced by the earthquake. Although the EQL approximation is simpler and time effective, the NL approach may yield more accurate results. In particular, the benefit of time domain NL schemes can be fully appreciated when the site is shaken by a strong seismic motion (e.g. Elia, 2014; Elia, Rouainia, Karofyllakis & Guzel, 2017).

This paper studies the influence of three different ideal soil deposits (with soil types B, C and D) on the response of the nonlinear one-bay 1-storey building via direct and decoupled SSI approaches. By complying with the EC8 prescription, seven outcrop input motions and surface input motions are scaled. Outcrop input motions are firstly processed through the soil deposits then applied to the fixed base structural model while the surface input motions are directly applied to the model. This paper proceeds by briefly describing the soil and building models. Subsequently, the scaled input motions are described. This is followed by the results and discussions. Finally, the summary of the study is presented with the outcomes.

2. FE soil models

An ideal soft clay soil deposit with 50 m depth and 5 m width is modelled in the fully-coupled finite element code SWANDYNE II (Chan, 1995). The soil column is discretised by 250, 1x1 m isoparametric quadrilateral finite elements with 8 solid nodes and 4 fluid nodes (Figure 1). This mesh generation ensures that the seismic wave transmission is represented accurately through the FE soil model (Bathe, 1982). During the dynamic analyses, the bottom of the mesh is assumed rigid at the bedrock, while the nodes along the vertical sides are characterized by the same displacements (i.e. tied-nodes lateral boundary conditions). The modified input motions are directly applied to the solid nodes at the base of the mesh as prescribed horizontal displacement time histories. The dynamic simulations are carried out with a time step corresponding to that of the earthquake input signals.

The advanced kinematic hardening soil model *RMW* (Rouainia & Wood, 2000) is used to simulate the dynamic soil behaviour during the nonlinear site response analyses. *RMW* has been successfully employed to predict the dynamic performance of different earth structures (Elia & Rouainia, 2013; Elia & Rouainia, 2014) as it can capture early irreversibility, accumulation of pore pressure, stiffness degradation and damping ratio curves and the destructure of soil under undrained conditions (Guzel, 2019). In this work, the soil material parameters are determined by conducting a series of undrained cyclic simple shear test

simulations (using a program called SM2D (Chan, 1995) under controlled strain levels in order to produce normalised shear modulus shown in Figure 1. The comparison with Vucetic and Dobry (1991) results indicates that the predicted response is within the range of the experimental data. The adopted *RMW* parameters are summarised in Table 1.

Table 1.

RMW model parameters calibrated against the nonlinear curves given by Vucetic and Dobry (1991)

λ^*	κ^*	M	ν	R	A*	B	k	ψ	r_o
0.2	0.02	1.	0.	0.	0.4	8.	0.	1.	1.
52	97	35	22	1	94	0	5	0	75

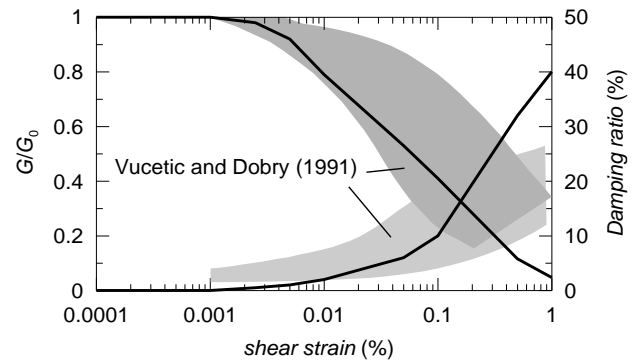


Figure 1. Shear stiffness degradation and corresponding damping ratio curves based on *RMW* model parameters.

The initial stiffness profiles of the soil deposit are attained using the equation (1) proposed by Viggiani and Atkinson (1995) for the dependency of the small-strain shear modulus, G_0 , on the mean effective stress and overconsolidation ratio (R_o):

$$\frac{G_0}{p_r} = A \left(\frac{p'}{p_r} \right)^n R_o^m \tag{1}$$

where p_r is a reference pressure equal to 1 kPa. In all cases, with respect to the plasticity index of 35, m and n in the equation are set equal to 0.27 and 0.84, respectively. With this set of m and n parameters, the dimensionless stiffness parameter A attained as 1050 so that the shear wave velocity at the top 30 m is consistent with the soil class of D (Guzel, Elia & Rouainia, 2017). In the same way, by keeping the m and n parameters constant, the values of A parameter are set to 1600 and 6500 for soil classes B and D, respectively. In the initialisation phases of the FE models, an overconsolidation ratio equals to, on average, the value of 1.5. The resulting shear wave velocity profiles (shown in Figure 2) have an average value at the top 30 m of the soil column equal to 540, 345 and 140 m/s, thus classifying the deposit as a soil class of B, C and D

according to EC8. Accordingly, the first natural periods (T_1) of the three soil deposits are equal to 0.3, 0.47 and 1.17 s, respectively.

small-strain range is compensated by the viscous damping.

3. Building model

An ideal one-bay, one-storey frame building model shown in Figure 3, with 11 m height and 12.8 m width, is simulated with OpenSees, following the example presented by Mazzoni, McKenna, Scott and Fenves (2006). Columns and beams have sections equal to 152.4 cm × 122 cm and 244 cm × 152.4 cm, respectively. The concrete and steel units of the reinforced concrete sections are defined as a single homogenised material. The model base nodes are fixed for the displacements and freed for the rotations. The frame noethides are free to displace and rotate. Beam and column elements are allowed to accommodate a nonlinear behaviour in accord with the defined moment-curvature relationship. In particular, flexural stiffness in elastic and inelastic regions are set to 894e4 (kNm²) and 574e4 (kNm²) while yield moment and yield curvature equal to 146.9e2 (kNm) and 0.256e-2 (1/m), respectively) with strain-hardening ratio of 0.01. Representative moment-curvature relationship is presented in Figure 4. Since the focus of this research is to study the influence of direct and decoupled approaches on the building responses, this given example is directly used. Although the physical dimensions of the model are not carefully considered, this will not change the overall conclusions of the work.

The fundamental period of the building model is equal to 1.17 s. Two additional frame models with fundamental periods of 0.9 s and 0.6 s are also considered by changing the mass of the building. This is to investigate the influence of the building fundamental period on the drift response of frame models with a similar shape. It is important to note here that the research and publishing ethics are adhered throughout the present paper.

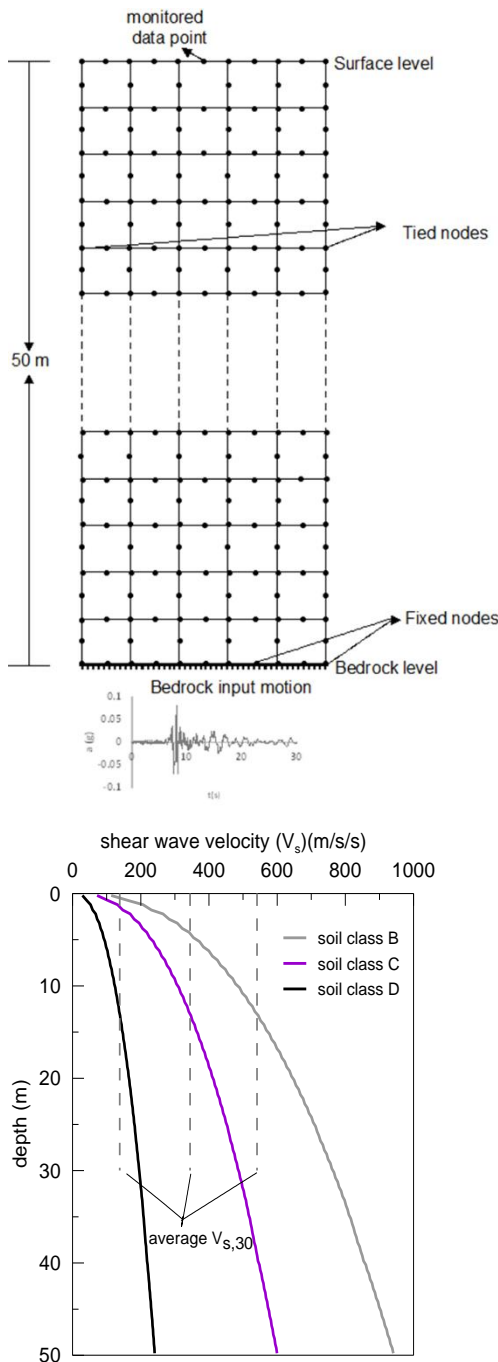


Figure 2. Model of the 50 m soil deposit and shear wave velocity profiles for soil classes B, C and D.

In the dynamic simulations conducted with SWANDYNE II, only 5%, 3% and 2% of Rayleigh damping for soil class B, C and D are introduced. This is to ensure that the propagation of spurious high frequencies are avoided and the RMW model underestimation of damping in the

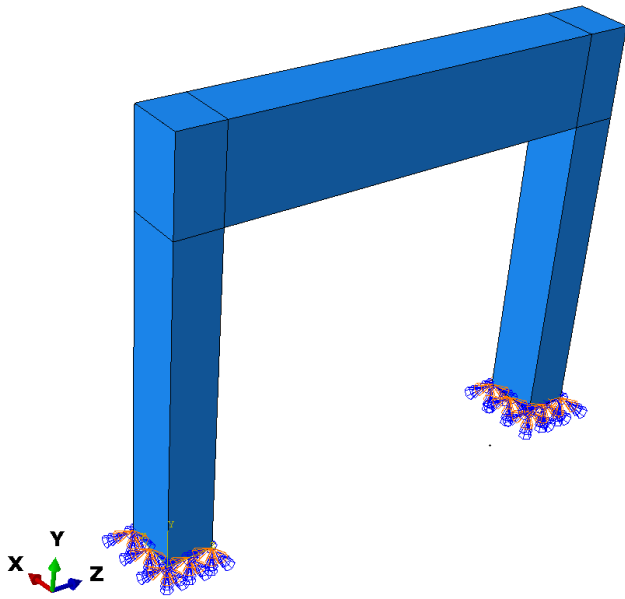


Figure 3. One-bay 1-storey frame building model modelled in OpenSees.

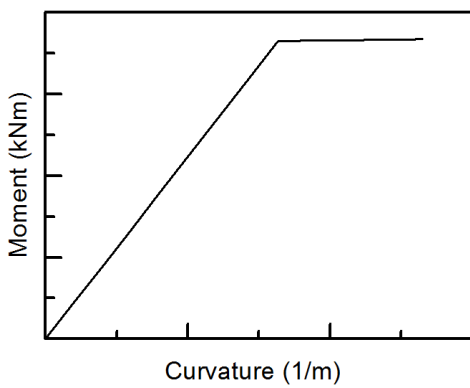


Figure 4. Representative moment-curvature relation adopted in this work.

4. Modification of Input Motions

Seven real surface input motions recorded on soil classes B, C and D and seven real input motions recorded at the outcropping rock (i.e. soil class A) are selected and modified to the associated EC8 design response spectra levels by using a computer program REXEL (Iervolino, Galasso & Cosenza, 2010), accounting for two seismic intensity levels (i.e. 0.15g and 0.35g). For the sake of brevity, general characteristics of earthquake events are presented in the Appendix 1. Since ideal soil sites are investigated in this study, magnitude and distance hazard contributions are selected to cover most of the earthquake recordings in the European Strong-motion Database (ESM). The input motions are scaled in such a way that the mean response spectrum of the seven earthquake records is within the 10% lower limits and 30% upper limits of the target response spectra (shown in Figure 5 and Figure 6).

The outcrop input motions can be vital in investigating the local site effects and in the nonlinear site response analysis. The outcrop input motions can be used as bedrock input motions in the site response analysis (Pinzón, Mánica, Pujades & Alva, 2019). In this study, the target response spectra is damped by 5% and have 2% of probability of exceedance in 50 years (i.e. 475 years of return period). It is important to note here that in order to account for the extraordinary earthquake scenarios, it is necessary to consider outcrop input motions with return periods of 2475 years (i.e. 50% of probability of exceedance in 50 years) (Tönük et.al., 2014).

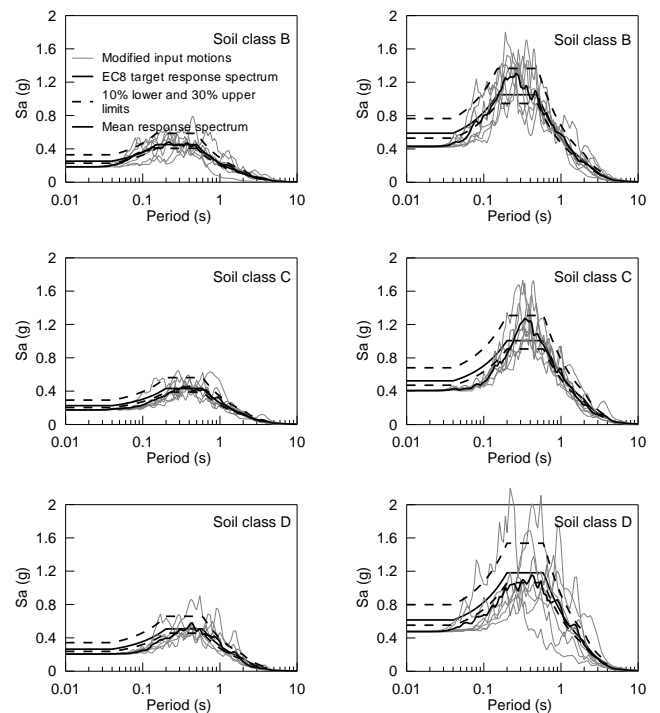


Figure 5. Spectral responses of seven modified surface input motions to the EC8 target response spectra for soil classes B, C and D at 0.15g (left figures) and 0.35g (right figures) seismic intensity levels.

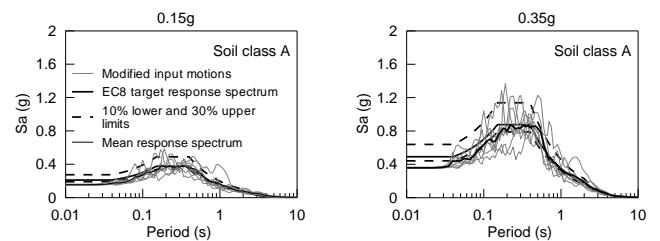


Figure 6. Spectral responses of seven modified outcrop input motions to the EC8 target response spectra of soil class A at 0.15g and 0.35g seismic intensity levels.

The modified surface input motions represented in Figure 5 are directly applied to the building model. The modified outcrop input motions shown in Figure 5 are

firstly propagated through the soil models, then, applied to the building model. The outcrop standard design spectrum is represented in Figure 6 with the legend of EC8 target response spectrum. It should be noted in here that processing the outcrop input motions through the soil deposits causes the spectral values to be underpredicted at periods less than 0.3 s (seen in Figure 7). This is more apparent at the higher seismic intensity level (i.e. 0.35g) attributing probably to the induced higher strains. Nevertheless, the nonlinear ground response analyses lead to better spectral predictions above the period of 0.3 s. These results are in line with the literature (Kaklamanos, Baise, Thompson & Dorfmann, 2015) and cannot bias the current work, as the periods of the building model are well above the underpredicted region in the spectral response curves.

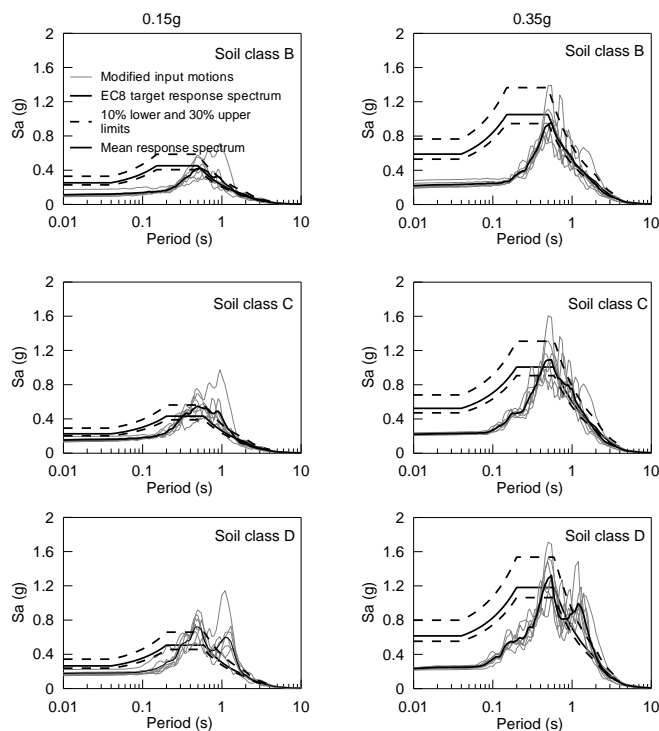


Figure 7. Spectral responses of processed input motions at 0.15g (left figures) and 0.35g (right figures) seismic intensity levels through the soil deposits classified with class B, C and D according to EC8 criterion.

5. Results

The response of one-storey one-bay structure model with first mode period of 1.17 s is represented in terms of drift response. Figure 8a and Figure 8b reports the drift responses of building under processed outcrop input motions (Case 1). Figure 8c and Figure 8d indicate the responses of the model under modified surface input motions recorded on soil classes B, C and D (Case 2). Additionally, Figure 9a and Figure 9b compares the medians of drift responses in Case 1 and Case 2 followed

by the standard deviation comparisons in Figure 9c and Figure 9d.

The drift responses in both Case 1 and Case 2 increase from stiffer soil (i.e. soil type B) to relatively softer soil (i.e., soil type D) with different levels of variability. This is correctly accounted for by the EC8 approach, which considers the influence of the soil deposit stiffness on the target response spectra by introducing a different soil factor for each soil class. Since the softer soil deposit has more impact on the spectral responses than the stiffer soil deposit (as also observed by Rey, Faccioli & Bommer, 2002), soil factors given by EC8 for softer soils is greater than stiffer soils. This means that the EC8 target response spectrum for soil class D has the greatest spectral values followed by the spectrum for soil type C and B, respectively. It is also obvious that, for the same soil deposit, the drift responses are higher at 0.35g seismic intensity level than at 0.15g seismic intensity level, both in Case 1 and Case 2.

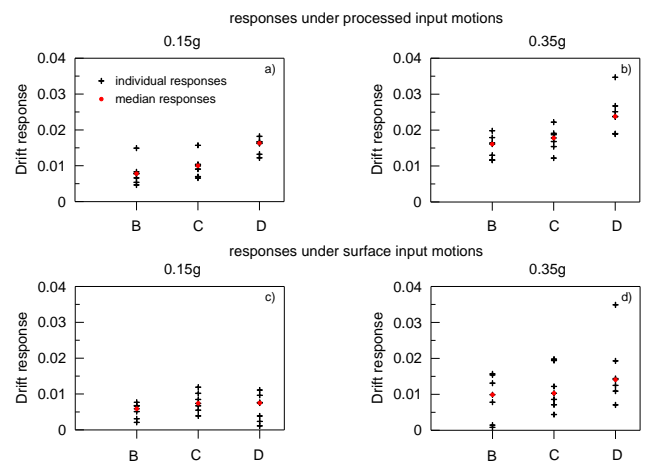


Figure 8. Drift responses of the building model with 1.17 s of first mode period on top of the ideal sites with soil classes B, C and D under; processed input motions (a, b) and surface input motions (c, d) at 0.15g and 0.35g seismic intensity levels.

Figure 8 also indicates that the median responses in Case 1 are greater than those obtained in Case 2. This is shown apparently in Figure 9a and in Figure 9b for the three types of soils. In terms of standard deviations (std) presented in Figure 9c and Figure 9d, modified surface input motions always lead to more scattered drift responses than those obtained under processed input motions at the higher seismic intensity level and at all soil types. However, this is not quite valid in case of the lower seismic intensity level, especially at soil types of B and C.

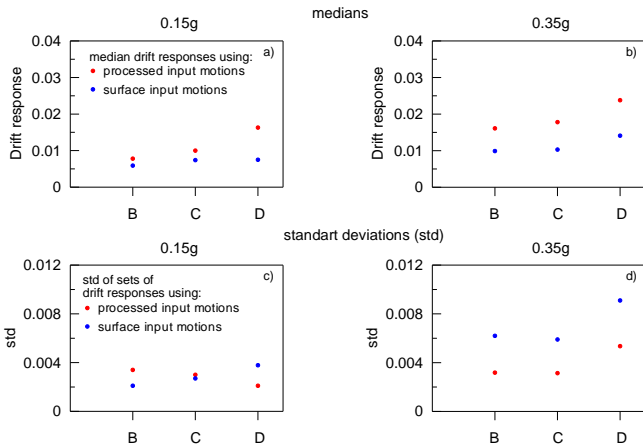


Figure 9. Comparisons of medians (a, b) and standard deviations (c, d) of the sets of drift responses shown in Figure 7 for three different soil types at 0.15g and 0.35g seismic intensity levels.

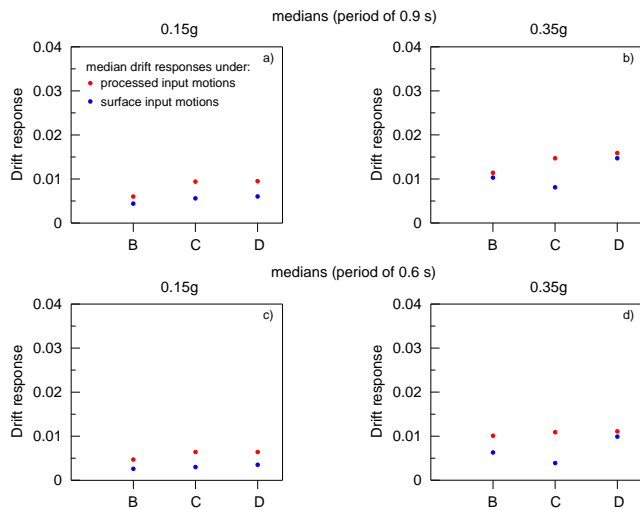


Figure 10. Comparisons of median drift responses of building models with first mode periods of 0.9 s (a, b) and 0.6 s (c, d) under processed input motions and surface input motions.

Finally, building models characterised by first mode periods of 0.9 s and 0.6 s are analysed accounting for the two SSI approaches, as seen in Figure 10 (a, b) and Figure 9 (c, d), respectively. It is, again, clear that the median drift responses under processed input motions are larger than those attained from the surface input motions for all three types of soils at both seismic intensity levels. The trend of drift responses getting greater towards the softer soil type is also observed in both building models, attributing to the relatively greater influence of the soft soil deposits on the surface input motions.

Figure 11 indicates median drift responses of the building models with three different first mode periods, 1.17 s, 0.9 s and 0.6 s under processed (a, b) and

modified surface (c, d) input motions. The shorter the building period, the lesser the median drift response is experienced by the model for each soil class and at both seismic intensity levels.

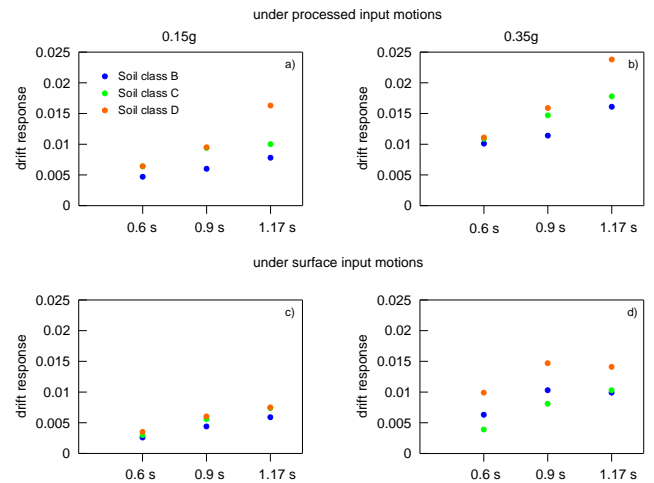


Figure 11. Median drift responses of building models with 0.6 s, 0.9 s and 1.17 s periods on top of the soil types of B, C and D under processed and surface input motions under 0.15g and 0.35g seismic intensity levels.

6. Conclusions

In this study, the seismic response of one-bay 1-storey building model is assessed via fixed-base and decoupled SSI approaches. In fixed-base approach, the model of the column bases are fixed and EC8-compliant selected input motions are applied. In decoupled approach, instead, the outcrop input motions are firstly selected and propagated through the soil columns (e.g. free-field soil deposits) by performing nonlinear site response analyses. Then, from site response analyses, surface input motions are attained. Ultimately, these surface input motions are applied to the building model. Three different soil classes of B, C and D and two seismic intensity levels (i.e. 0.15g and 0.35g) are considered in both approaches.

The main conclusions of the work are;

- The building response depends directly on the applied seismic input motions and it increases with the increase of seismicity level.
- There is also strong dependency of drift responses to the fundamental period of the building model. Building model having higher period tends to experience higher horizontal displacements.
- The drift responses of the model become larger when the decoupled approach is adopted. Hence, the decoupled approach can result in more conservative design of buildings. In particular, this approach can be appreciated when buildings are situated on softer soil deposits, where greater level of nonlinearity is accumulated.

- The stiffer the soil deposit, the lesser the building model can induce the drift response. This finding justifies the reason of engineering practitioner's intention of preferring stiff soil deposits underneath building foundations.

Author contributions

Contributions of Yusuf GÜZEL; soil modelling, nonlinear site response analyses, writing of the original draft, Fidan GÜZEL; input motion selections, building model and analyses.

Conflict of Interest

The authors, hereby, declare no conflict of interest.

References

- Amirzehni, E., Taiebat, M., Finn, W. L., & DeVall, R. H. (2015). Ground motion scaling/matching for nonlinear dynamic analysis of basement walls. In *Proceedings of the 11th Canadian Conference on Earthquake*. Victoria: BC, Canada. Retrieved from https://www.caee.ca/pdf/Paper_98723.pdf
- Ancheta, T. D., Darragh, R. B., Stewart, J. P., Seyhan, E., Silva, W. J., Chiou, B. S. J., ... & Donahue, J. L. (2013). PEER NGA-West2 Database (PEER Report No. 2013/03). Pacific Earthquake Engineering Research Center. University of California, Berkeley. Retrieved from https://apps.peer.berkeley.edu/publications/peer_reports/reports_2013/webPEER-2013-03-Ancheta.pdf
- Bathe, K.J. (1982). *Finite element procedures in engineering analysis*. New Jersey: Prentice Hall.
- CEN. (2005). *Eurocode 8: Design of structures for earthquake resistance – Part 1: General rules, seismic actions and rules for buildings*. Brussels.
- Chan AHC. (1993). *User manual for DIANA SWANDYNE-II*. School of Civil Engineering, University of Birmingham.
- Elia, G. (2015). Site Response for Seismic Hazard Assessment. *Encyclopedia of Earthquake Engineering*. doi:http://dx.doi.org/10.1007/978-3-642-36197-5_241-1
- Elia, G., & Rouainia, M. (2013). Seismic performance of earth embankment using simple and advanced numerical approaches. *Journal of Geotechnical and Geoenvironmental Engineering*, 139(7), 1115-1129. doi:[http://dx.doi.org/10.1061/\(ASCE\)GT.1943-5606.0000840](http://dx.doi.org/10.1061/(ASCE)GT.1943-5606.0000840)
- Elia, G., & Rouainia, M. (2014). Performance evaluation of a shallow foundation built on structured clays under seismic loading. *Bulletin of Earthquake Engineering*, 12(4), 1537-1561. doi:<http://dx.doi.org/10.1007/s10518-014-9591-3>
- Elia, G., Rouainia, M., Karofyllakis, D., & Guzel, Y. (2017). Modelling the non-linear site response at the LSST down-hole accelerometer array in Lotung. *Soil Dynamics and Earthquake Engineering*, 102, 1-14. doi:<http://dx.doi.org/10.1016/j.soildyn.2017.08.007>
- Galasso, C., & Iervolino, I. (2011). Relevant and minor criteria in real record selection procedures based on spectral compatibility. In *Proceedings of the 14th conference ANIDIS "L'ingegneria sismica in Italia"*. Bari (Italy). Retrieved from http://wpage.unina.it/iuniervo/papers/Galasso_Iervolino_ANIDIS_2011.pdf
- Gokhan, D. O. K., Ozturk, H., & Demir, A. (2017). Determining moment-curvature relationship of reinforced concrete columns. *The Eurasia Proceedings of Science Technology Engineering and Mathematics*, (1), 52-58. Retrieved from <http://www.epstem.net/en/download/article-file/379911>
- Guzel, Y. (2019). *Influence of input motion selection and soil variability on nonlinear ground response analyses (Doctoral dissertation)*. Newcastle University. Retrieved from <http://theses.ncl.ac.uk/jspui/handle/10443/4436>
- Guzel, Y., Elia, G., & Rouainia, M. (2017). The effect of input motion selection strategies on nonlinear ground response predictions. In *COMPdyn 2017-Proceedings of the 6th International Conference on Computational Methods in Structural Dynamics and Earthquake Engineering* (pp. 3739-3747). Rhodes Island (GR): National Technical University of Athens. doi:<http://dx.doi.org/10.7712/120117.5679.17209>
- Hancock, J., Watson-Lamprey, J., Abrahamson, N. A., Bommer, J. J., Markatis, A., McCoy, E. M. M. A., & Mendis, R. (2006). An improved method of matching response spectra of recorded earthquake ground motion using wavelets. *Journal of Earthquake Engineering*, 10(spec01), 67-89. doi:<https://doi.org/10.1080/13632460609350629>
- Iervolino, I., & Manfredi, G. (2008). A review of ground motion record selection strategies for dynamic structural analysis. *Modern Testing Techniques for Structural Systems*, 131-163. doi:http://dx.doi.org/10.1007/978-3-211-09445-7_3
- Iervolino, I., Galasso, C., & Cosenza, E. (2010). REXEL: computer aided record selection for code-based seismic structural analysis. *Bulletin of Earthquake Engineering*, 8(2), 339-362. doi:<http://dx.doi.org/10.1007/s10518-009-9146-1>
- Kaklamanos, J., Baise, L. G., Thompson, E. M., & Dorfmann, L. (2015). Comparison of 1D linear, equivalent-linear, and nonlinear site response models at six KiK-net validation sites. *Soil Dynamics and*

Earthquake Engineering, 69, 207-219.
doi:<https://doi.org/10.1016/j.soildyn.2014.10.016>

Kottke, A., & Rathje, E. M. (2008). A semi-automated procedure for selecting and scaling recorded earthquake motions for dynamic analysis. *Earthquake Spectra*, 24(4), 911-932.
doi:<http://dx.doi.org/10.1193/1.2985772>

Kramer, S. L. (1996). *Geotechnical earthquake engineering*. New Jersey: Prentice Hall.

Mazzoni, S., Hachem, M., & Sinclair, M. (2012). An improved approach for ground motion suite selection and modification for use in response history analysis. In XV World Conference on Earthquake Engineering, Lisboa. Retrieved from https://www.iitk.ac.in/nicee/wcee/article/WCEE2012_5752.pdf

Mazzoni, S., McKenna, F., Scott, M. H., & Fenves, G. L. (2006). *OpenSees command language manual*. Pacific Earthquake Engineering Research (PEER) Center, 264, 137-158. Retrieved from <https://opensees.berkeley.edu/OpenSees/manuals>

Pinzón, L.A., Mánica, M.A., Pujades, L.G. & Alva, R.E., 2020. Dynamic soil-structure interaction analyses considering directionality effects. *Soil Dynamics and Earthquake Engineering*, 130, 106009.
doi:<http://dx.doi.org/10.1016/j.soildyn.2019.106009>

Pitilakis, K., Riga, E., & Anastasiadis, A. (2012). Design spectra and amplification factors for Eurocode 8. *Bulletin of Earthquake Engineering*, 10(5), 1377-1400. doi:<http://dx.doi.org/10.1007/s10518-012-9367-6>

Pitilakis, K., Riga, E., & Anastasiadis, A. (2013). New code site classification, amplification factors and normalized response spectra based on a worldwide ground-motion database. *Bulletin of Earthquake Engineering*, 11(4), 925-966. doi:<http://dx.doi.org/10.1007/s10518-013-9429-4>

Rathje, E. M., Kottke, A. R., & Trent, W. L. (2010). Influence of input motion and site property variabilities on seismic site response analysis. *Journal of Geotechnical and Geoenvironmental Engineering*, 136(4), 607-619.

doi:[http://dx.doi.org/10.1061/\(ASCE\)GT.1943-5606.0000255](http://dx.doi.org/10.1061/(ASCE)GT.1943-5606.0000255)

Rey, J., Faccioli, E., & Bommer, J. J. (2002). Derivation of design soil coefficients (S) and response spectral shapes for Eurocode 8 using the European Strong-Motion Database. *Journal of Seismology*, 6(4), 547-555. Retrieved from <https://link.springer.com/article/10.1023/A:1021169715992>

Roesset, J. M. (1977). Soil amplification of earthquakes. *Numerical Methods in Geotechnical Engineering*, 639-682. Retrieved from <https://ci.nii.ac.jp/naid/10007803851/>

Rouainia, M., & Muir Wood, D. (2000). A kinematic hardening constitutive model for natural clays with loss of structure. *Géotechnique*, 50(2), 153-164.
doi:<http://dx.doi.org/10.1680/geot.2000.50.2.153>

Shome, N., Cornell, C. A., Bazzurro, P., & Carballo, J. E. (1998). Earthquakes, records, and nonlinear responses. *Earthquake Spectra*, 14(3), 469-500.
doi:<http://dx.doi.org/10.1193/1.1586011>

Stewart, J.P. (2008). Benchmarking of nonlinear geotechnical ground response analysis procedure. Pacific Earthquake Engineering Research Center (NTIS issue no. 201212). University of California, Berkeley. Retrieved from <https://ntrl.ntis.gov/NTRL/dashboard/searchResults/titleDetail/PB2012106298.xhtml>

Tönük, G., Ansal, A., Kurtuluş, A., & Çetiner, B. (2014). Site specific response analysis for performance based design earthquake characteristics. *Bulletin of Earthquake Engineering*, 12(3), 1091-1105.
doi:<http://dx.doi.org/10.1007/s10518-013-9529-1>

Viggiani, G., & Atkinson, J. H. (1995). Stiffness of fine-grained soil at very small strains. *Géotechnique*, 45(2), 249-265.
doi:<http://dx.doi.org/10.1680/geot.1995.45.2.249>

Vucetic, M., & Dobry, R. (1991). Effect of soil plasticity on cyclic response. *Journal of Geotechnical Engineering*, 117(1), 89-107.
doi:[http://dx.doi.org/10.1061/\(ASCE\)0733-9410\(1991\)117:1\(89\)](http://dx.doi.org/10.1061/(ASCE)0733-9410(1991)117:1(89))

Appendix-1

Table 1. General properties of earthquake events adopted in the selection and modification of input motions at 0.15g seismicity levels.

Soil Class	Earthquake Name	Date	Mw	Fault Mechanism	Epicentral Distance [km]	PGA_X [m/s ²]	PGA_Y [m/s ²]	PGV_X [m/s]	PGV_Y [m/s]
A	Campano Lucano	11/23/1980	6.9	normal	25	0.588	0.588	0.044	0.059
	Kalamata	10/13/1997	6.4	thrust	61	0.205	0.201	0.015	0.015
	Kalamata	10/13/1997	6.4	thrust	103	0.126	0.113	0.013	0.011
	Mt. Vatnafjoll	5/25/1987	6	oblique	42	0.138	0.131	0.010	0.012
	Bingol	5/1/2003	6.3	strike slip	14	5.051	2.918	0.336	0.210
	Izmit	8/17/1999	7.6	strike slip	47	2.334	1.328	0.221	0.125
	Montenegro	4/15/1979	6.9	thrust	21	1.774	2.199	0.171	0.259
B	South of Vathi	11/5/1997	4.6	?	163	0.128	0.106	0.009	0.008
	Kalamata	9/13/1986	5.9	normal	11	2.354	2.670	0.315	0.235
	Montenegro (aftershock)	5/24/1979	6.2	thrust	20	0.560	0.543	0.036	0.043
	Manesion	6/7/1989	5.2	oblique	24	0.265	0.254	0.026	0.022
	Aigion (aftershock)	6/15/1995	5.6	oblique	34	0.103	0.093	0.010	0.011
	Strofades	11/18/1997	6.6	oblique	38	1.289	1.135	0.109	0.078
	Montenegro	4/15/1979	6.9	thrust	16	3.680	3.557	0.421	0.520
C	Griva	12/21/1990	6.1	normal	51	0.059	0.081	0.009	0.009
	Adana	6/27/1998	6.3	strike slip	30	2.158	2.644	0.278	0.203
	Ionian	11/4/1973	5.8	thrust	15	5.146	2.498	0.570	0.255
	Friuli (aftershock)	9/15/1976	6	thrust	9	1.069	0.932	0.108	0.112
	Manjil	6/20/1990	7.4	oblique	81	0.951	0.842	0.116	0.153
	Komilion	2/25/1994	5.4	oblique	15	1.307	1.345	0.103	0.119
	Campano Lucano	11/23/1980	6.9	normal	137	0.372	0.311	0.084	0.072
D	Duzce 1	11/12/1999	7.2	oblique	174	0.1844	0.223	0.039	0.021
	Griva	12/21/1990	6.1	normal	66	0.0566	0.1011	0.004	0.012
	Kalamata	9/13/1986	5.9	normal	10	2.1082	2.9095	0.327	0.323
	Kalamata	9/13/1986	5.9	normal	11	2.3537	2.6703	0.315	0.235
	South Iceland (aftershock)	6/21/2000	6.4	strike slip	14	1.7476	1.1423	0.097	0.177
	Adana	6/27/1998	6.3	strike slip	30	2.1575	2.6442	0.278	0.203
	Montenegro	4/15/1979	6.9	thrust	16	3.6801	3.5573	0.421	0.52

Table 2. General properties of earthquake events adopted in the selection and modification of input motions at 0.35g seismicity levels.

Soil Class	Earthquake Name	Date	Mw	Fault Mechanism	Epicentral Distance [km]	PGA_X [m/s ²]	PGA_Y [m/s ²]	PGV_X [m/s]	PGV_Y [m/s]
A	Campano Lucano	11/23/1980	6.9	normal	25	0.588	0.588	0.044	0.059
	Kalamata	10/13/1997	6.4	thrust	61	0.205	0.201	0.015	0.015
	Izmit (aftershock)	9/13/1999	5.8	oblique	15	0.714	3.112	0.055	0.145
	Vrancea	8/30/1986	7.2	thrust	49	0.823	1.408	0.151	0.132
	Campano Lucano	11/23/1980	6.9	normal	32	2.121	3.166	0.330	0.553
	Bingol	5/1/2003	6.3	strike slip	14	5.051	2.918	0.336	0.210
	Izmit	8/17/1999	7.6	strike slip	78	0.512	1.040	0.043	0.149
B	South of Vathi	11/5/1997	4.6	?	163	0.128	0.106	0.009	0.008
	Kalamata	9/13/1986	5.9	normal	11	2.354	2.670	0.315	0.235
	Montenegro (aftershock)	5/24/1979	6.2	thrust	20	0.560	0.543	0.036	0.043
	Umbria Marche	9/26/1997	6	normal	38	0.897	0.948	0.136	0.176
	Strofades	11/18/1997	6.6	oblique	38	1.289	1.135	0.109	0.078
	Gulf of Akaba	11/22/1995	7.1	oblique	93	0.783	0.894	0.099	0.104
	Campano Lucano	11/23/1980	6.9	normal	33	0.968	0.975	0.134	0.068
C	Duzce 1	11/12/1999	7.2	oblique	174	0.184	0.223	0.039	0.021
	Griva	12/21/1990	6.1	normal	66	0.057	0.101	0.004	0.012
	Kalamata	9/13/1986	5.9	normal	10	2.108	2.910	0.327	0.323
	Kalamata	9/13/1986	5.9	normal	11	2.354	2.670	0.315	0.235
	South Iceland (aftershock)	6/21/2000	6.4	strike slip	14	1.748	1.142	0.097	0.177
	Duzce 1	11/12/1999	7.2	oblique	8	3.699	5.036	0.357	0.635
	Montenegro	4/15/1979	6.9	thrust	16	3.680	3.557	0.421	0.520
D	Strofades (aftershock)	11/18/1997	6	strike slip	160	0.146	0.128	0.015	0.012
	Duzce 1	11/12/1999	7.2	oblique	174	0.184	0.223	0.039	0.021
	Adana	6/27/1998	6.3	strike slip	30	2.158	2.644	0.278	0.203
	Ionian	11/4/1973	5.8	thrust	15	5.146	2.498	0.570	0.255
	Kalamata	9/13/1986	5.9	normal	10	2.108	2.910	0.327	0.323
	Kalamata	9/13/1986	5.9	normal	10	2.108	2.910	0.327	0.323
	Montenegro	4/15/1979	6.9	thrust	16	3.680	3.557	0.421	0.520